GRADUATE AERONAUTICAL LABORATORIES
CALIFORNIA INSTITUTE OF TECHNOLOGY

Arbocz, J. and Babcock, C.D.

A Multimode Analysis for Calculating Buckling Loads of Imperfect Cylindrical Shells. June, 1974
C.I.T SM 74-4

Firestone Flight Sciences Laboratory

Guggenheim Aeronautical Laboratory

Karman Laboratory of Fluid Mechanics and Jet Propulsion

Pasadena

SM 74-4

A MULTIMODE ANALYSIS FOR CALCULATING BUCKLING LOADS OF IMPERFECT CYLINDRICAL SHELLS

by

Johann Arbocz and C. D. Babcock, Jr.

California Institute of Technology

Pasadena, California

June 1974

This work was supported by the National Science Foundation under Grant GK 16934. This aid is gratefully acknowledged.

TABLE OF CONTENTS

A MULTIMODE ANALYSIS FOR CALCULATING BUCKLING LOADS OF IMPERFECT CYLINDRICAL SHELLS

by

Johann Arbocz and C. D. Babcock, Jr.

ABSTRACT

By expanding the response of a cylindrical shell in truncated Fourier series, the nonlinear Donnell type shell equations for imperfect stiffened shells were reduced to a set of linear equations in the correction terms by Newton's method of quasilinearization. Solutions were obtained for isotropic and for ring and stringer stiffened shells. The amplitudes of the initial imperfections used in the analysis were calculated from the corresponding Imbert-Donnell imperfection models. The free parameters in this imperfection model were obtained by least square fitting the harmonics of the experimentally measured initial imperfections. It was possible in all cases to achieve satisfactory correlation using only a few suitably chosen deflection and imperfection modes.

ACKNOWLEDGEMENT

The authors wish to thank Prof. E. E. Sechler, whose support and encouragement made this work possible. The excellent drawings of Mrs. Betty Wood and the skillful typing by Mrs. Elizabeth Fox are very much appreciated.

This work was supported by NSF through Grant GK 16934. This aid is gratefully acknowledged.

NOMENCLATURE

c	-	Poisson's effect ($c = \sqrt{3(1-\nu^2)}$)
D	-	bending stiffness ($D = \frac{Et^3}{4c^2}$)
D_{xx}, D_{xy}, D_{yy}	-	effective bending stiffnesses - see Reference 11
E	-	Young's modulus (lb/in^2)
$F, F_{io}, F_{k\ell}, F'_{k\ell}$	-	Airy stress functions
$\delta F, \delta F_{io}, \delta F_{k\ell}, \delta F'_{k\ell}$	-	stress function correction terms - see eqs. 7 and 14
H_{xx}, H_{xy}, H_{yy}	-	effective stretching stiffnesses - see Reference 11
i, k	-	number of half waves in the axial direction
ℓ	-	number of full waves in the circumferential direction
L	-	shell length (in)
L_D, L_H, L_Q	-	linear operators defined by eqs. 3, 4 and 5 respectively
L_{NL}	-	nonlinear operator defined by eq. 6
M_x	-	moment resultant (in lb/in)
N_x	-	stress resultant (lb/in)
R	-	radius of shell (in)
Q_{xx}, Q_{xy}, Q_{yy}	-	effective torsional stiffnesses - see Reference 11
q, r, s	-	parameters determined from least square fit - see Reference 28
t	-	thickness of shell (in)
S, T	-	dummy arguments used in eq. 6
u, v, w	-	displacement components in the x, y and z directions, respectively
$W, W_{io}, W_{k\ell}, W'_{k\ell}$	-	radial displacements - positive inward
$\delta W, \delta W_{io}, \delta W_{k\ell}, \delta W'_{k\ell}$	-	radial displacement correction terms - see eqs. 7 and 13

NOMENCLATURE (Cont'd)

$\overline{W}_{io}, \overline{W}_{k\ell}, \overline{W}'_{k\ell}$	-	radial imperfections from perfect circular cylinder
λ	-	nondimensional loading parameter ($\lambda = \frac{cR}{t} \frac{\sigma}{E}$)
$\lambda_{c\ell}$	-	classical buckling load
λ_s	-	axial load level at the limit point of an imperfect cylinder
ρ	-	nondimensional loading parameter for stiffened shells ($\rho = \frac{N_x}{N_{x_{c\ell}}}$)
ν	-	Poisson's ratio
$\overline{\xi}$	-	initial imperfection amplitude

INTRODUCTION

The buckling behavior of axially compressed thin walled stiffened or unstiffened cylindrical shells has been a major concern to practicing structural engineers for many years. Initial geometrical imperfections have been accepted qualitatively as the explanation for the discrepancy between the analytical predictions and the experimental values and for the frequently large scatter of the experimental results. This acceptance is mainly due to the work of a few investigators[1, 2, 3] who, using specialized imperfections, have demonstrated the sensitivity of the buckling load to initial imperfections.

However, despite the accepted theoretical explanation of the buckling behavior of axially compressed shells, the incorporation of the idea of imperfection sensitivity into engineering practice has not been accomplished except in an empirical manner. The engineers who design actual shell structures against buckling do it by the method developed in the early 40's[4, 5] by using an empirical "knockdown factor" applied to the results of the classical small deflection theory. The "knockdown factor" is chosen so that its product with the classical buckling load leads to a lower bound to all the experimental data for the shell-loading configuration under consideration.

This apparent reluctance of the practicing structural engineers to accept and assimilate the findings of the theoreticians is based on two often overlooked but very important facts. In the first place, with the exception of a few papers by Hutchinson[6], Thurston and Freeland[7], and Arbocz and Babcock[8], the bulk of the imperfection studies deal with idealized axisymmetric shapes which are seldom,

if ever, realized in the actual shell structures. The other, and from the designer's standpoint probably the more important reason, is the complete absence of measurement of imperfections for full-scale structures.

For laboratory scale shell structures, imperfections have been measured by the Galcit group for several years[8, 9]. Buckling load predictions based on these imperfections have been published previously[8, 10]. These imperfection correlation studies were based on approximate solutions of the Donnell type imperfect shell equations. These solutions did not satisfy the correct experimental boundary conditions. In the present work, special attention has been paid to account for the effects of the nonlinear prebuckling deformations due to the edge constraints and the correct experimental boundary conditions.

EFFECT OF GENERAL IMPERFECTIONS - MULTIMODE SOLUTION

The correlation studies reported in this paper were carried out using an analytical solution of the imperfect shell equations that can incorporate general imperfection shapes. Initially the nonlinear Donnell type shell equations are reduced to a set of linear partial differential equations by Newton's method of quasilinearization. (This type of solution was first applied to the imperfect shell problem by Thurston and Freeland[7].) A combination of Fourier expansion and Galerkin's procedure then results in a set of algebraic equations in terms of the harmonic components of the correction terms. Finally, the system of algebraic equations is solved by a standard iterative procedure.

Stiffened Shell Equations

Using the sign convention defined in Fig. 1 the Donnell type equations for imperfect stiffened cylindrical shells can be written[11]

$$L_H(F) - L_Q(W) = -\frac{1}{R} W,_{xx} - \tfrac{1}{2} L_{NL}(W, W+2\overline{W}) \tag{1}$$

$$L_Q(F) + L_D(W) = \frac{1}{R} F,_{xx} + L_{NL}(F, W+\overline{W}) \tag{2}$$

where the linear operators are

$$L_D(\ ) = D_{xx}(\ ),_{xxxx} + D_{xy}(\ ),_{xxyy} + D_{yy}(\ ),_{yyyy} \tag{3}$$

$$L_H(\ ) = H_{xx}(\ ),_{xxxx} + H_{xy}(\ ),_{xxyy} + H_{yy}(\ ),_{yyyy} \tag{4}$$

$$L_Q(\ ) = Q_{xx}(\ ),_{xxxx} + Q_{xy}(\ ),_{xxyy} + Q_{yy}(\ ),_{yyyy} \tag{5}$$

and the nonlinear operator is

$$L_{NL}(S, T) = S,_{xx}\, T,_{yy} - 2S,_{xy}\, T,_{xy} + S,_{yy}\, T,_{xx} \tag{6}$$

Commas in the subscripts denote repeated partial differentiation with respect to the independent variables following the comma. The stiffener properties have been "smeared out" to arrive at effective bending, stretching and torsional stiffnesses. The stiffener parameters D_{xx}, H_{xx}, Q_{xx}, D_{xy},... etc., are defined in Reference 11. These equations were first derived by Geier[12], however in the present notation they are due to Singer[13] and Hutchinson and Amazigo[14]. Here $\overline{W}$ is the initial radial imperfection, W is the component of displacement normal to the shell midsurface and F is the Airy stress function.

Newton's Method of Quasilinearization

Let us represent the $(m+1)^{th}$ approximation to a solution of eqs. 1 and 2 by

$$W_{m+1} = W_m + \delta W_m$$
$$F_{m+1} = F_m + \delta F_m \tag{7}$$

where

W_m, F_m = m^{th} approximation to the solution

δW_m, δF_m = correction to the m^{th} approximation

Substituting into eqs. 1 and 2 and neglecting squares of the correction quantities yields the following set of linear equations for determining the correction terms

$$L_H(\delta F_m) - L_Q(\delta W_m) + \frac{1}{R}\delta W_{m,xx} + L_{NL}(W_m + \overline{W}, \delta W_m) = -E_m^{(1)} \tag{8}$$

$$L_Q(\delta F_m) + L_D(\delta W_m) - \frac{1}{R}\delta F_{m,xx} - L_{NL}(F_m, \delta W_m) - L_{NL}(W_m + \overline{W}, \delta F_m) = -E_m^{(2)} \tag{9}$$

where

$$E_m^{(1)} = L_H(F_m) - L_Q(W_m) + \frac{1}{R}W_{m,xx} + \tfrac{1}{2}L_{NL}(W_m, W_m + 2\overline{W}) \tag{10}$$

$$E_m^{(2)} = L_Q(F_m) + L_D(W_m) - \frac{1}{R}F_{m,xx} - L_{NL}(F_m, W_m + \overline{W}) \tag{11}$$

Reduction to a Set of Algebraic Equations

If we represent the initial imperfections by

$$\overline{W} = t \sum_{i=1}^{N_1}{}' \overline{W}_{io} \cos i\bar{x} + t \sum_{k,\ell=1}^{N_2}{}'' \overline{W}_{k\ell} \sin k\bar{x} \cos \ell\bar{y}$$

$$+t \sum_{k,\ell=1}^{N_3}{}'' \overline{W}'_{k\ell} \sin k\bar{x} \sin \ell\bar{y} \qquad (12)$$

where $\bar{x} = \frac{\pi x}{L}$, $\bar{y} = \frac{y}{R}$

then eqs. 1 and 2 admit separable solutions of the form

$$\begin{Bmatrix} W_m \\ \delta W_m \end{Bmatrix} = t \begin{Bmatrix} W_\nu \\ 0 \end{Bmatrix} + t \sum_{i=1}^{N_1}{}' \begin{Bmatrix} W_{io} \\ \delta W_{io} \end{Bmatrix} \cos i\bar{x} + t \sum_{k,\ell=1}^{N_2}{}'' \begin{Bmatrix} W_{k\ell} \\ \delta W_{k\ell} \end{Bmatrix} \sin k\bar{x} \cos \ell\bar{y} \qquad (13)$$

$$+ t \sum_{k,\ell=1}^{N_3}{}'' \begin{Bmatrix} W'_{k\ell} \\ \delta W'_{k\ell} \end{Bmatrix} \sin k\bar{x} \sin \ell\bar{y}$$

$$\begin{Bmatrix} F_m \\ \delta F_m \end{Bmatrix} = \frac{ERt^2}{2} \begin{Bmatrix} -\frac{\lambda^2}{2} \bar{y}^2 \\ 0 \end{Bmatrix} + \frac{ERt^2}{c} \sum_{i=1}^{N_1}{}' \begin{Bmatrix} F_{io} \\ \delta F_{io} \end{Bmatrix} \cos i\bar{x} \qquad (14)$$

$$+ \frac{ERt^2}{c} \sum_{k,\ell=1}^{N_2}{}'' \begin{Bmatrix} F_{k\ell} \\ \delta F_{k\ell} \end{Bmatrix} \sin k\bar{x} \cos \ell\bar{y} + \frac{ERt^2}{c} \sum_{k,\ell=1}^{N_3}{}'' \begin{Bmatrix} F'_{k\ell} \\ \delta F'_{k\ell} \end{Bmatrix} \sin k\bar{x} \sin \ell\bar{y}$$

where

$$W_\nu = -\frac{\nu}{c} \frac{\overline{H}_{xx}}{1+\mu_1} \lambda \qquad c = \sqrt{3(1-\nu^2)}$$

The unknown coefficients are determined by Galerkin's procedure yielding a set of linear algebraic equations in terms of the unknown correction terms. In matrix notation

$$[I]\ \{\delta F\} + [C]\ \{\delta W\} = -\{E^{(1)}\} \tag{15}$$

$$[A]\ \{\delta F\} + [B]\ \{\delta W\} = -\{E^{(2)}\} \tag{16}$$

The terms of the coefficient matrices and the error vectors are written out in Appendix A.

To obtain the buckling load for a given imperfect cylindrical shell one begins by making an initial guess for $\{W\}$ and $\{F\}$ at a small initial load level λ. Iteration is then carried out until the correction vectors are smaller than some preselected value. The converged solutions then are used as the initial guess at the next higher axial load level $\lambda + \Delta\lambda$. The entire process is repeated for increasing values of the axial load parameter λ. The nonlinear analysis then will locate the limit point of the prebuckling states. By definition the value of the loading parameter λ corresponding to the limit point will be the theoretical buckling load.

It is shown in Appendix B that the solution satisfies the circumferential periodicity condition.

COMPARISON WITH OTHER SOLUTIONS

In order to assess the accuracy of the multimode solutions, comparisons with Koiter's asymptotic theory and with a numerical solution, which include rigorous satisfaction of the experimental boundary conditions, were carried out.

Koiter's Asymptotic Theory

It was pointed out by Koiter[15] that if for an isotropic shell the initial imperfections are represented by the following 3 modes

$$\overline{W} = t\overline{\xi}\left\{\cos i_{c\ell}\overline{x} + \sqrt{2}\, i_{c\ell}/k_1 \sin k_1 \overline{x} \cos \ell\overline{y} - \sqrt{2}\, i_{c\ell}/k_2 \sin k_2 \overline{x} \cos \ell\overline{y}\right\} \tag{17}$$

where

$$i_{c\ell} = \frac{L}{\pi}\sqrt{\frac{2c}{Rt}} \tag{18}$$

and k_1 and k_2 are the two roots of the quadratic equation

$$k^2 \frac{Rt}{2c}\left(\frac{\pi}{L}\right)^2 + \ell^2 \frac{Rt}{2c}\left(\frac{1}{R}\right)^2 - k\sqrt{\frac{Rt}{2c}}\,\frac{\pi}{L} = 0 \tag{19}$$

then buckling occurs by reaching a limit point at an axial load level λ_s given by the equation

$$(\lambda_s - 1)^2 = -6c\overline{\xi}\lambda_s \tag{20}$$

This result and the results using the multimode solution are given in Fig. 2. As can be seen, the multimode solution agrees with Koiter's asymptotic formula for sufficiently small values of the imperfection amplitude $\overline{\xi}$. However, for increasing values of $\overline{\xi}$ the multimode solution, which includes higher order terms in the approximate solution, predicts lower buckling loads. It should also be noticed that the imperfection represented by a suitable combination of the buckling modes is far more adverse than a single axisymmetric imperfection[2].

The Effects of Boundary Conditions and Nonlinear Prebuckling Deformations

The effect of experimental boundary conditions has been extensively discussed by Almroth[16], Hoff and Soong[17], and Weller, et al.[18]. The effects can be separated into two major items that will be discussed separately. These are the effect of nonlinear prebuckling deformation caused by the end constraint of the test shell and the effect of end fixity on the buckling deformation (eigenfunction) and its associated buckling load (eigenvalue).

The multimode analysis neglects completely the effect of the nonlinear prebuckling deformation caused by the edge constraint. The boundary conditions satisfied for the eigenvalue problem are the classical simple support conditions SS-3 ($w = M_x = v = N_x = 0$). In order to assess the difference in buckling load due to these effects, the BOSOR[19] and SRA[20] computer codes were used. Two isotropic, two stringer stiffened and two ring stiffened shells were used in this study. The properties of these shells are given in Table I. Initially the perfect shell behavior will be discussed.

Our study recovered the results of previous investigators[21, 22, 23], who showed that the buckling load of a moderate length perfect isotropic shell with a membrane prebuckling state is insensitive to boundary conditions, provided the out-of-plane deflection w and the in-plane circumferential displacement v are suppressed. The buckling load (expressed in lb/in) is always very close to the classical value:

$$N_{c\ell} = \frac{Et^2}{R\sqrt{3(1-\nu^2)}} \qquad (21)$$

If, however, one includes the nonlinear prebuckling deformations caused by the end constraints in the analysis, then the buckling load depends on the boundary conditions of the problem. For the SS-3 condition ($w = M_x = v = N_x = 0$) the load is reduced by about 16%, for the C-3 condition ($w = w_x = v = u = 0$) by about 7%. These results are given in detail in Table II.

For the lightly ring stiffened shells studied in this paper, the buckling load with membrane prebuckling, like for the isotropic shells, varies only slightly with the different boundary conditions. The inclusion of the nonlinear prebuckling deformations caused by the end constraints in the analysis results in an 8% decrease in the buckling load for the weak (SS-3) boundary condition; however, this effect is considerably less (about 1%) for the stiffer (C-3 and C-4) boundary conditions. These results are also given in Table II.

Finally, for the stringer stiffened shells studied, it is found that, contrary to the behavior of the isotropic and the lightly ring stiffened shells, the buckling load with membrane prebuckling depends strongly on the boundary conditions specified. Stiffening the boundary condition raises the buckling load by about 12% for C-3, by about 39% for the C-4 boundary condition. On the other hand, the inclusion of the nonlinear prebuckling deformation (with the shell loaded through the skin midsurface) has an insignificant effect.

From the results displayed in Table II, it appears that for perfect shells the nonlinear prebuckling deformation is important only for the isotropic shell and for the lightly ring stiffened shell with the weak (SS-3) boundary condition. On the other hand, boundary conditions (with membrane prebuckling) will only have a

significant effect for the stringer stiffened shell.

In order to investigate the behavior of shells with initial imperfections, an analysis developed by Arbocz[24], which takes into account both effects, will be used. In this analysis, the nonlinear partial differential equations are reduced to a set of nonlinear ordinary differential equations by a two mode circumferential expansion and a Galerkin procedure. The resulting nonlinear ordinary differential equations are solved numerically by a parallel shooting technique. This analysis, in which arbitrary imperfections (with appropriate circumferential dependence) and arbitrary boundary conditions can be accounted for, will be referred to as the "extended" analysis. In order to reduce the computer cost with the numerical analysis, the test shells were slightly shortened in length for this investigation. The properties of the shells X-1, XR-1 and XS-1 are listed in Table I.

First we shall examine the effect of an idealized imperfection, consisting of an axisymmetric and an asymmetric mode, on the buckling load of an isotropic shell. Thus, for

$$\overline{W} = -0.5\ t \cos 2\overline{x} + 0.05\ t \sin \overline{x} \cos 13\ \overline{y} \qquad (22)$$

it was found that the multimode and the extended analysis with C-3 boundary conditions gave virtually the same buckling load[25]. The results are displayed in Fig. 3, where in addition to a load-displacement relationship the deformations near the maximum load level as computed by the two analyses are displayed. It is clear from this figure that despite the complete difference in edge constraint (and hence in the deformation near the shell edges) the imperfection is dominant and

it controls the behavior of the shell. This implies that for dominant imperfections the nonlinear prebuckling deformation due to end constraint can be neglected.

Investigating the effect of an idealized imperfection consisting of one axisymmetric and two asymmetric modes on the buckling load of a lightly ring stiffened shell, good agreement was found between the results of the multimode and the extended analysis with C-3 boundary conditions[26]. As can be seen from Table III, the difference in the critical load predicted by the two analyses is approximately 1%.

When working with the stringer stiffened shell XS-1, one must remember that for the perfect shell the buckling load depends strongly on the specified boundary conditions. Thus, using an idealized imperfection consisting of one axisymmetric and one asymmetric imperfection, it was found that the multimode and the extended analysis with SS-3 boundary conditions gave virtually the same buckling load[26]. Notice also from the results displayed in Table III that the imperfection resulted in a 38% decrease in the buckling load when compared with the analysis using a membrane prebuckling state and the same SS-3 boundary conditions. Next we calculated the buckling load of the same shell with the same initial imperfections but with C-3 boundary conditions. This resulted in a 37% decrease in the buckling load when compared with the analysis using a membrane prebuckling state and the same C-3 boundary conditions. This similarity in the reduction of the buckling load for the two boundary conditions motivated the decision to take boundary conditions into account (when they are

important) by comparing the imperfect shell buckling load to the corresponding perfect shell buckling load using in both cases the same boundary conditions. This procedure will be followed in the correlation study with experimentally measured initial imperfections. It should be noted that in this study this will be necessary only for the stringer stiffened shell.

THE AVERAGED IMPERFECTION MODEL

The correlation studies to be carried out using the previously described multimode analysis require the measured initial imperfections in the form of double Fourier expansions. The measurements were taken by equipment specifically designed for this purpose at GALCIT and the results are reported in the literature[8, 9, 27]. The amplitudes of the Fourier coefficients are calculated from the measured data in a standard manner. When observing such data displayed on a log-log basis[27] it is evident that the imperfection amplitude coefficient can be approximated by straight lines as follows:

$$\overline{W}_{io} = \frac{\overline{X}_A}{i^q} \qquad \overline{W}_{k\ell} = \frac{\overline{X}}{k^r \ell^s} \tag{25}$$

where

$\overline{W}_{io}$ is the amplitude of the i^{th} axisymmetric Fourier harmonic,

$\overline{W}_{k\ell}$ is the amplitude of the k, ℓ^{th} asymmetric Fourier harmonic and

$\overline{X}_A, \overline{X}, q, r, s$ are coefficients determined by least-square fitting the measured data.

This model, introduced by Imbert[28] following an idea by Donnell and Wan[1] was extensively utilized by Arbocz and Babcock[10] in previous

correlation studies. The same imperfection model will be used in this study for the following reasons.

In the first place, the correlation studies carried out in this paper required in some cases imperfection amplitudes at wave numbers that were not measured. This was due to the fact that in the early experimental work the experimental data spacing was not sufficiently close to resolve all the harmonic amplitudes of interest. Therefore, the imperfection model was fitted over the wave numbers actually measured and then the amplitudes of the harmonics of interest could be obtained by extrapolation. The accuracy of this procedure is unknown. Secondly, the imperfection model fitting is a numerical smoothing operation of the experimental data. It was felt that such an operation was desirable due to the experimental scatter experienced in obtaining the imperfection measurements. Thirdly, it is highly desirable to have an imperfection model that represents a class of shells manufactured by a given process. The utilization of the imperfection sensitivity calculations will undoubtedly occur before the detailed shell imperfections are available. Therefore it is necessary to make predictions based on an imperfection model of this type. The parameters of the imperfection model used in this study are given in Table IV.

MODE SELECTION

The number of modes of deformation included in the analysis is limited by practical considerations, like the available core size and the time required for obtaining the solution. Thus, since the shell buckling load will be determined from the governing equations by using a particular set of modes, an attempt at optimizing the selection of these modes must be made. That is, we want to locate those modes which dominate the prebuckling and buckling behavior of the shell.

Examples of attempts to locate "critical modes," defined as that combination of axisymmetric and asymmetric modes which would yield the lowest buckling load, have been reported by Arbocz and Babcock[8, 10, 11] and Imbert[28]. These imperfection studies have shown that in order to yield a decrease from the buckling load of the perfect shell the initial imperfection harmonics used must include at least one mode with a significant initial amplitude and an associated eigenvalue that is close to the buckling load of the perfect shell. Hence, in this investigation, the selection of modes will be based on the following three considerations:

1. the eigenvalue of the mode,
2. the initial amplitude of the mode,
3. the coupling of the mode selected with other modes of the solution.

Based on the modes selected, the theoretical buckling load will be calculated. Different combinations will be used in order to investigate the influence of wave numbers and initial amplitudes on the

calculated buckling load. Finally the lowest buckling load calculated will be compared with the experimentally determined buckling loads.

Eigenvalue Maps and Initial Imperfection Amplitudes

Figures 4, 5 and 6 show maps of the classical buckling loads for three of the experimental shells used in this investigation. The buckling loads were calculated for a perfect shell using membrane prebuckling and classical simply supported boundary conditions ($w = M_x = v = N_x = 0$).

For the isotropic shell A-8, the lowest buckling load ($\rho = 1.0$) is a multiple eigenvalue occurring for a family of modes. We know from previous correlation studies[8, 10] that at least one of these modes should be included in the assumed solution. Also, as can be seen from Fig. 4 there are many modes whose eigenvalue is only slightly higher than the lowest eigenvalue $\rho = 1.0$.

For the ring stiffened shell AR-1, the lowest eigenvalue ($\rho = 1.0$) is single valued and is associated with a short wavelength axisymmetric mode. Once again there are several modes whose eigenvalue is only slightly higher than the lowest eigenvalue. However, it is clear from the results of Fig. 5 that the ring stiffened shell AR-1 has only a few modes with eigenvalues less than or equal to 1.01 (within 1% of the lowest eigenvalue $\rho = 1.0$) and that all these modes have short wavelength in the axial direction. It should also be noticed that the first asymmetric mode with one half wave in the axial direction has an associated eigenvalue of 1.5 (50% higher than the lowest eigenvalue $\rho = 1.0$).

The lowest eigenvalue ($\rho = 1.0$) of the stringer stiffened shell

AS-2 is also single valued but it is associated with an asymmetric mode that has one half wave in the axial direction. Also, as can be seen from Fig. 6, there are only 3 modes with eigenvalues less than 1.10 (within 10% of the lowest eigenvalue $\rho = 1.0$). As a matter of fact there are only a few modes with eigenvalues less than 1.50.

The amplitudes of the initial imperfections used in the correlation studies are computed from the averaged imperfection model. This analytical imperfection model, which expresses the variation of the imperfection amplitudes with axial and circumferential wave number, combined with the eigenvalue maps provide the investigator with a very useful guide when selecting the modes to be included in the analysis. A relatively large initial amplitude, combined with a mode shape whose eigenvalue is close to the lowest value, will always result in a buckling load which is lower than the classical value.

Coupling of Modes

By definition one or more modes are coupled, if their inclusion in the analysis results in nonzero off-diagonal terms in the matrices C, A and B of eqs. 15 and 16. (The first matrix is a diagonal matrix.) It can be shown that coupling between one axisymmetric mode with wave numbers (i, o) and 2 asymmetric modes with wave numbers (k, ℓ) and (m, n) will occur, if the relation $i = |k \pm m|$ and $\ell = n$ are satisfied. For the degenerate case of 1 axisymmetric (i, o) and 1 asymmetric mode (k, ℓ) the coupling conditions reduce to the single relation $i = 2k$[8]. Further it has been found that coupling between 3 asymmetric modes with wavenumbers

(k, ℓ), (m, n) and (p, q) will occur if the relations $k \pm m \pm p$ = odd integer and $q = |\ell \pm n|$ are satisfied. If these coupling conditions are satisfied, then the resulting buckling load of the shell is generally lower than the buckling load when each mode is considered separately.

IMPERFECTION CORRELATION STUDIES

Next the experimental buckling loads of the shells A-8, B-1, AR-1 and AS-2 were predicted by using some of the mode shape combinations found previously to have important coupling properties. The experimentally determined averaged imperfection model was used in this study.

The buckling load calculations for shell A-8 are summarized in Table V. In this table the notation (2, 0) denotes an axisymmetric mode with 2 half waves in the axial direction, whereas (1, 9) stands for an asymmetric mode with a single half wave in the axial direction and 9 full waves in the circumferential direction. The fundamental role that the basic combination (2, 0) + (1, 9) + (33, 9) + (34, 0) plays becomes evident as more and more modes are included in the solution. The importance of the basic combination is explained by the fact that as shown in Fig. 7, the 3 modes (1, 9), (33, 9) and (34, 0) lie on the Koiter circle associated with the lowest eiganvalue $\rho = 1.0$. The results of Table V indicate that in going from a 6-mode to a 10-mode solution the addition of 4 new modes resulted in a 9% decrease in the predicted buckling load, whereas the inclusion of 5 additional modes (15-mode solution) resulted only in a further 1/2% decrease. This behavior suggests that there is a point beyond which the addition of more modes will not necessarily result in further significant

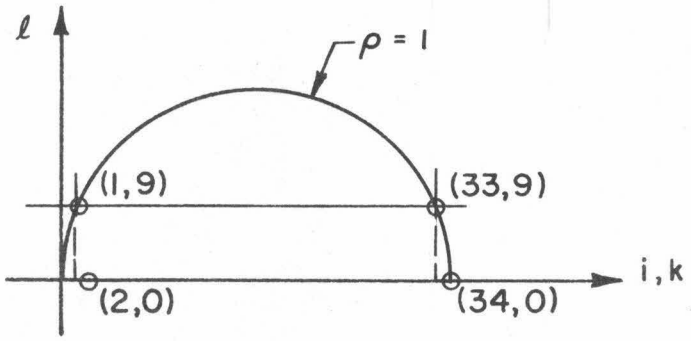

Fig. 7 Basic Combination on the Koiter Circle

decrease of the predicted buckling load. The buckling load calculations for the isotropic shell B-1, summarized in Table VI, followed the same general pattern.

The buckling load calculations for the ring stiffened shell AR-1 are summarized in Table VII. The selection of the modes follows the same pattern as for the isotropic shells A-8 and B-1. However, in this case the inclusion of additional modes results in only relatively small decreases in the predicted buckling loads. The reason for this behavior becomes evident if one considers the distribution of the eigenvalues for the shell AR-1 shown in Fig. 5. All those modes whose associated eigenvalues are close to the lowest eigenvalue have many half waves in the axial direction. Thus their initial amplitudes, as given by eq. 25 of the averaged imperfection model are very small. Conversely, the associated eigenvalues of the modes with significant initial amplitudes (modes with few half waves in the

axial direction) are considerably higher than the lowest eigenvalue. Thus their contribution to the lowering of the calculated buckling loads is ineffective.

The buckling load calculations for the stringer stiffened shell AS-2 are summarized in Table VIII. Comparing the result of the 2-mode solution with that of the 4-mode solution, it is evident that the additional short wavelength modes have only an insignificant effect. The reason for this becomes immediately evident if one considers the distribution of the eigenvalues for the shell AS-2 shown in Fig. 6. Only the eigenvalues of a few asymmetric modes with long wavelength in the axial direction are close to the lowest eigenvalue, which in this case is asymmetric. Coupling of these modes resulted in a significant decrease in the predicted buckling load. The insignificant effect of the short wavelength axial modes is further illustrated by the fact that the elimination of these modes from the 14 mode solution resulted in a buckling load of $\rho = 0.828$, only slightly higher than the value of $\rho = 0.824$ predicted by the 14 mode solution itself.

Finally, in Table IX, the lowest buckling loads predicted by the multimode solutions are compared with the corresponding experimental values. The agreement is very good for the isotropic shells A-8 and B-1 and satisfactory for the ring and stringer stiffened shells AR-1 and AS-2.

CONCLUSIONS

The main conclusion that can be drawn from this investigation is that, with the proposed multimode analysis, it is possible to predict reasonably well the buckling load of axially compressed isotropic and stiffened shells from measured initial imperfections.

Further, from the detailed imperfection correlation studies one must conclude that, if realistic variation of the imperfection amplitudes with wavelength is taken into account, then suitable combinations of axisymmetric and asymmetric modes are always more damaging than either a single axisymmetric or a single asymmetric mode.

The proposed multimode analysis does not include the effect of the prebuckling deformations caused by the edge constraints. However, comparisons with the so-called "extended" analysis that includes such effects have shown that prebuckling deformations are unimportant in the presence of reasonably sized imperfections which tend to dominate the shell response, if the resulting deformations are symmetric with respect to the mid-plane of the shell. It was also found that the importance of the different boundary conditions can be properly assessed by the linear theory using membrane prebuckling solutions, and whenever the boundary conditions are important they can be taken into account by proper normalizing. These conclusions concerning the influence of the edge condition are based upon a limited investigation but appear to substantiate standard engineering practice.

Finally, it is also abundantly clear that the further incorporation of imperfection sensitivity ideas into engineering practice will have to await the measurements of imperfections of full scale structures and subsequent correlation studies.

REFERENCES

1. Donnell, L. M. and Wan, C. C., "Effect of Imperfections on Buckling of Thin Cylinders and Columns under Axial Compression, J. Appl. Mech., Vol. 17, 1950, p. 73.

2. Koiter, W. T., "The Effect of Axisymmetric Imperfections on the Buckling of Cylindrical Shells under Axial Compression," Koninkl. Ned. Akad. Weterschap Proc. B. 66, pp. 265-279, 1963.

3. Budiansky, B. and Hutchinson, J. W., "Dynamic Buckling of Imperfection-Sensitive Structures," Proc. XI Intern. Congr. Appl. Mech., Edited by H. Görtler, Springer Verlag, Berlin, 1964, pp. 636-651.

4. Kanemitsu, S. and Nojima, N. M., "Axial Compression Tests of Thin Circular Cylinders," M.S. Thesis, California Institute of Technology, 1939.

5. NASA Space Vehicle Design Criteria (Structures), NASA SP-8007, Revised, August 1968.

6. Hutchinson, J. W., "Axial Buckling of Pressurized Imperfect Cylindrical Shells," AIAA J., Vol. 3, No. 8, pp. 1461-1466, August 1965.

7. Thurston, G. A. and Freeland, M. A., "Buckling of Imperfect Cylinders under Axial Compression," NASA CR-541, July 1966.

8. Arbocz, J. and Babcock, C. D., "The Effect of General Imperfections on the Buckling of Cylindrical Shells," J. Appl. Mech., Vol. 36, No. 1, pp. 28-38, March 1969.

9. Singer, J., Arbocz, J., and Babcock, C. D., "Buckling of Imperfect Stiffened Cylindrical Shells under Axial Compression," AIAA J., Vol. 9, No. 1, pp. 68-75, January 1971.

10. Arbocz, J. and Babcock, C. D., "On the Role of Imperfections in Shell Buckling," (Paper presented at the 13th IUTAM Congress in Moscow, Aug. 21-26, 1972.) Also GALCIT Report SM 72-4.

11. Arbocz, J., "The Effect of Initial Imperfections on Shell Stability," in Thin-Shell Structures, edited by Y. C. Fung and E. E. Sechler, Prentice-Hall, 1974.

12. Geier, B., "Das Beulverhalten Versteifter Zylinderschalen Teil 1, Differential-Gleichungen," Z. Flugwiss, Vol. 14, pp. 306-323, July 1966.

13. Singer, J., Personal Communication, 1968.

REFERENCES (Cont'd)

14. Hutchinson, J. W. and Amazigo, J. C., "Imperfection Sensitivity of Eccentrically Stiffened Cylindrical Shells," AIAA J., Vol. 5, No. 3, pp. 392-401, March 1967.

15. Koiter, W. T., Personal Communication, California Institute of Technology, April 1974.

16. Almroth, B. O., "Influence of Edge Conditions on the Stability of Axially Compressed Cylindrical Shells," NASA CR-161, February 1965.

17. Hoff, N. J. and Soong, T. E., "Buckling of Circular Cylindrical Shells in Axial Compression," SUDAER No. 204, Stanford, California, August 1964.

18. Weller, T., Singer, J. and Batterman, S. C., "Influence of Eccentricity of Loading on Buckling of Stringer-Stiffened Cylindrical Shells," Proc. of the Thin Shell Structures Symposium, Prentice-Hall, 1974, pp. 305-324.

19. Bushnell, D., Almroth, B. O. and Sobel, L. H., "Buckling of Shells of Revolution with Various Wall Construction," Vol. 3. User's Manual for BOSOR, NASA CR-1051, 1968.

20. Cohen, G. A., "Buckling of Axially Compressed Cylindrical Shells with Ring Stiffened Edges." AIAA J., Vol. 4, No. 10, Oct. 1966, pp. 1859-1862.

21. Ohira, H., "Local Buckling Theory of Axially Compressed Cylinders," Proc. of the Eleventh Japan National Congress for Applied Mechanics, 1961.

22. Hoff, N. J., "Buckling of Thin Shells," Proc. of an Aerospace Symposium of Distinguished Lecturers in Honor of Dr. Theodore von Karman on his 80th Anniversary. The Institute of Aerospace Sciences, New York, 1961.

23. Yamaki, N. and Kodama, S., "Buckling of Circular Cylindrical Shells under Compression/Report 2, Solutions Based on the Flügge Equations Neglecting Prebuckling Edge Rotations. Rep. Inst. High Speed Mech., Japan, Vol. 24, 1971.

24. Arbocz, J., "Buckling of Axially Compressed Imperfect Cylindrical Shells," Proc. of the AIAA/ASME 12th Structures, Structural Dynamics and Materials Conference, Anaheim, California, April 19-21, 1971.

25. Arbocz, J. and Sechler, E. E., "On the Buckling of Axially Compressed Imperfect Cylindrical Shells." J. Appl. Mech., Vol. 41, No. 3, pp. 737-743, September 1974.

26. Arbocz, J. and Sechler, E. E., "On the Buckling of Axially Compressed Ring- and Stringer-Stiffened Imperfect Cylindrical Shells," GALCIT Report SM 73-10, California Institute of Technology, December 1973.

27. Babcock, C. D., "Experiments in Shell Buckling," in Thin-Shell Structures, edited by Y. C. Fung and E. E. Sechler, Prentice-Hall, 1974.

28. Imbert, J., "The Effect of Imperfections on the Buckling of Cylindrical Shells," Aeronautical Engineer Thesis, California Institute of Technology, June 1971.

APPENDIX A

DISCRETIZATION OF THE GOVERNING EQUATIONS

Substituting the double Fourier series used for representing the initial imperfection $\overline{W}$ (12), the radial displacement W with its correction δW (13) and the stress function F with its correction δF (14) into the compatibility and equilibrium equations 8 and 9, using standard trigonometric identities and regrouping, yields the "ERRORS" ϵ_{N_1} and ϵ_{N_2}. These "ERRORS" are functions of the unknown correction terms used in the above-mentioned double Fourier series. Finally these unknown correction terms are determined by solving the sets of simultaneous algebraic equations obtained by evaluating the integrals listed below. These integrals result from applying Galerkin's idea of minimization to the "ERRORS" ϵ_{N_1} and ϵ_{N_2}. Thus we get from the Compatibility Equation:

$$\int_0^{2\pi R}\int_0^{L} \epsilon_{N_1} \cos\frac{i\pi x}{L}\,dxdy = 0 \qquad \text{for } i = 1,2,\ldots,N_1 \qquad (A\text{-}1)$$

$$\int_0^{2\pi R}\int_0^{L} \epsilon_{N_1} \sin\frac{k\pi x}{L}\cos\frac{\ell y}{R}\,dxdy = 0 \qquad \text{for } k = 1,2,\ldots,N_2 \qquad (A\text{-}2)$$

$$\int_0^{2\pi R}\int_0^{L} \epsilon_{N_1} \sin\frac{k'\pi x}{L}\sin\frac{\ell' y}{R}\,dxdy = 0 \qquad \text{for } k' = 1,2,\ldots,N_3 \qquad (A\text{-}3)$$

and from the Equilibrium Equation:

$$\int_0^{2\pi R}\int_0^{L} \epsilon_{N_2} \cos\frac{i\pi x}{L}\,dxdy = 0 \qquad \text{for } i = 1,2,\ldots,N_1 \qquad (A\text{-}4)$$

$$\int_0^{2\pi R}\int_0^{L} \epsilon_{N_2} \sin\frac{k\pi x}{L}\cos\frac{\ell y}{R}\,dxdy = 0 \qquad \text{for } k = 1,2,\ldots,N_2 \qquad (A\text{-}5)$$

$$\int_0^{2\pi R}\int_0^{L} \epsilon_{N_2} \sin\frac{k'\pi x}{L}\sin\frac{\ell' y}{R}\,dxdy = 0 \qquad \text{for } k' = 1,2,\ldots,N_3 \qquad (A\text{-}6)$$

In matrix notation the resulting equations can be written as follows:

$$\begin{bmatrix} I_i & 0 & 0 \\ 0 & I_k & 0 \\ 0 & 0 & I_{k'} \end{bmatrix} \begin{Bmatrix} \delta F_{io} \\ \delta F_{k\ell} \\ \delta F'_{k\ell} \end{Bmatrix} + \begin{bmatrix} C_{i,i} & C_{i,k} & C_{i,k'} \\ C_{k,i} & C_{k,m} & C_{k,m'} \\ C_{k',i} & C_{k',m} & C_{k',m'} \end{bmatrix} \begin{Bmatrix} \delta W_{io} \\ \delta W_{k\ell} \\ \delta W'_{k\ell} \end{Bmatrix} = - \begin{Bmatrix} E^{(1)}_{io} \\ E^{(1)}_{k\ell} \\ E^{(1)}_{k'\ell'} \end{Bmatrix} \qquad (A\text{-}7)$$

$$\begin{bmatrix} A_{i,i} & A_{i,k} & A_{i,k'} \\ A_{k,i} & A_{k,m} & A_{k,m'} \\ A_{k',i} & A_{k',m} & A_{k',m'} \end{bmatrix} \begin{Bmatrix} \delta F_{io} \\ \delta F_{k\ell} \\ \delta F'_{k\ell} \end{Bmatrix} + \begin{bmatrix} B_{i,i} & B_{i,k} & B_{i,k'} \\ B_{k,i} & B_{k,m} & B_{k,m'} \\ B_{k',i} & B_{k',m} & B_{k',m'} \end{bmatrix} \begin{Bmatrix} \delta W_{io} \\ \delta W_{k\ell} \\ \delta W'_{k\ell} \end{Bmatrix} = - \begin{Bmatrix} E^{(2)}_{io} \\ E^{(2)}_{k\ell} \\ E^{(2)}_{k'\ell'} \end{Bmatrix} \qquad (A\text{-}8)$$

where I_i, I_k and $I_{k'}$ are N_1, N_2 and N_3 dimensional UNIT matrices respectively.

Repeated subscripts denote DIAGONAL matrices and the individual BLOCK matrices are given by the following formulas:

$$A_{i,i} = \frac{2R}{t}\left(\overline{Q}_{xx}\, a_i^2 + 1\right)$$

$$B_{i,i} = a_i^2\, \overline{D}_{xx} - 2\lambda \qquad \text{(A-9)}$$

$$C_{i,i} = -\frac{1}{2}\,\frac{t}{R}\,\frac{\left(\overline{Q}_{xx} a_i^2 + 1\right)}{a_i^2\, \overline{H}_{xx}} \qquad \text{where } i = 1, 2, \ldots, N_1$$

$$A_{i,k} = c\frac{R}{t}\left\{ \sum_{m,n=1}^{N_2}{}' \beta_n^2 (W_{mn} + \overline{W}_{mn})(\delta_{i=k+m} - \delta_{i=|k-m|})\delta_{n=\ell} \right\}$$

$$B_{i,k} = c\frac{R}{t}\left\{ \sum_{m,n=1}^{N_2} \beta_n^2\, F_{mn}(\delta_{i=k+m} - \delta_{i=|k-m|})\, \delta_{n=\ell} \right\} \qquad \text{(A-10)}$$

$$C_{i,k} = -\frac{1}{4}\,\frac{t}{R}\,\frac{c}{\overline{H}_{xx}}\,\frac{1}{a_i^2}\left\{ \sum_{m,n=1}^{N_2}{}' \beta_n^2 (W_{mn} + \overline{W}_{mn})(\delta_{i=k+m} - \delta_{i=|k-m|})\delta_{n=\ell} \right\}$$

$$\text{where } i = 1, 2, \ldots, N_1$$

$$k = 1, 2, \ldots, N_2$$

$$A_{i,k'} = c\frac{R}{t}\left\{ \sum_{p,q=1}^{N_3}{}' \beta_q^2 (W'_{pq} + \overline{W}'_{pq})(\delta_{i=k'+p} - \delta_{i=|k'-p|})\delta_{q=\ell'} \right\}$$

$$B_{i,k'} = c\frac{R}{t}\left\{ \sum_{p,q}^{N_3}{}' \beta_q^2 F'_{pq}\, (\delta_{i=k'+p} - \delta_{i=|k'-p|})\delta_{q=\ell'} \right\} \qquad \text{(A-11)}$$

$$C_{i,k'} = -\frac{1}{4}\,\frac{t}{R}\,\frac{c}{\overline{H}_{xx}}\,\frac{1}{a_i^2}\left\{ \sum_{p,q=1}^{N_3}{}' \beta_q^2 (W'_{pq} + \overline{W}'_{pq})(\delta_{i=k'+p} - \delta_{i=|k'-p|})\delta_{q=\ell'} \right\}$$

$$\text{where } i = 1, 2, \ldots, N_1$$

$$k' = 1, 2, \ldots, N_3$$

$$E_{io}^{(1)} = -\left\{ -\frac{1}{8}\frac{t}{R}\frac{c}{\overline{H}_{xx}}\frac{1}{\alpha_i^2}\left\langle \sum_{k,\ell=1}^{N_2}\sum W_{k\ell}\left\{ \sum_{p,q=1}^{N_2}\sum \beta_q^2 (W_{pq}+2\overline{W}_{pq})(\delta_{i=k+p}-\delta_{i=|k-p|})\delta_{q=\ell}\right\}\right\rangle \right.$$

$$-\frac{1}{8}\frac{t}{R}\frac{c}{\overline{H}_{xx}}\frac{1}{\alpha_i^2}\left\langle \sum_{k,\ell'=1}^{N_3}\sum W'_{k\ell}\left\{ \sum_{p,q=1}^{N_3}\sum \beta_q^2 (W'_{pq}+2\overline{W}'_{pq})(\delta_{i=k'+p}-\delta_{i=|k'-p|})\delta_{q=\ell'}\right\}\right\rangle$$

$$\left. +F_{io} - \frac{1}{2}\frac{t}{R}\frac{(\overline{Q}_{xx}\alpha_i^2+1)}{\alpha_i^2\overline{H}_{xx}} W_{io}\right\} \qquad (A-12)$$

$$E_{io}^{(2)} = -\left\{ c\frac{R}{t}\left\langle \sum_{k,\ell=1}^{N_2}\sum F_{k\ell}\left\{ \sum_{p,q=1}^{N_2}\sum \beta_q^2 (W_{pq}+\overline{W}_{pq})(\delta_{i=k+p}-\delta_{i=|k-p|})\,\delta_{q=\ell}\right\}\right\rangle \right.$$

$$+ c\frac{R}{t}\left\langle \sum_{k',\ell'=1}^{N_3}\sum F'_{k\ell}\left\{ \sum_{p,q=1}^{N_3}\sum \beta_q^2 (W'_{pq}+\overline{W}'_{pq})(\delta_{i=k'+p}-\delta_{i=|k'-p|})\delta_{q=\ell'}\right\}\right\rangle$$

$$\left. + 2\frac{R}{t}(\overline{Q}_{xx}\alpha_i^2+1)F_{io}+\alpha_i^2\overline{D}_{xx}W_{io}-2\lambda(W_{io}+\overline{W}_{io})\right\} \qquad (A-13)$$

where $i = 1, 2, \ldots, N_1$

$$A_{k,i} = -2c\frac{R}{t}\alpha_i^2\left\{ \sum_{p,q=1}^{N_2}\sum \beta_q^2 (W_{pq}+\overline{W}_{pq})(\delta_{k=i+p}-\delta_{k=|i-p|})\,\delta_{q=\ell}\right\}$$

$$B_{k,i} = -2c\frac{R}{t}\alpha_i^2\left\{ \sum_{p,q=1}^{N_2}\sum \beta_q^2 F_{pq}(\delta_{k=i+p}-\delta_{k=|i-p|})\,\delta_{q=\ell}\right\} \qquad (A-14)$$

$$C_{k,i} = \frac{c}{2}\frac{t}{R}\alpha_i^2\frac{1}{\overline{\gamma}_{H,k,\ell}}\left\{ \sum_{p,q=1}^{N_2}\sum \beta_q^2 (W_{pq}+\overline{W}_{pq})(\delta_{k=i+p}-\delta_{k=|i-p|})\,\delta_{q=\ell}\right\}$$

where $i = 1, 2, \ldots, N_1$

$k = 1, 2, \ldots, N_2$

$$A_{k,m} = A'_{k,m} + A''_{k,m} + A_{k,k}\,\delta_{k=m}$$

$$B_{k,m} = B'_{k,m} + B''_{k,m} + B_{k,k}\,\delta_{k=m} \qquad (A-15)$$

$$C_{k,m} = C'_{k,m} + C''_{k,m} + C_{k,k}\,\delta_{k=m}$$

where

$$A'_{k,m} = -2c\,\frac{R}{t}\,\beta_n^2\left\{\sum_{i=1}^{N_1} a_i^2(W_{io}+\overline{W}_{io})(\delta_{k=i+m}-\delta_{k=|i-m|})\right\}\delta_{n=\ell}$$

$$B'_{k,m} = -2c\,\frac{R}{t}\,\beta_n^2\left\{\sum_{i=1}^{N_1} a_i^2 F_{io}(\delta_{k=i+m}-\delta_{k=|i-m|})\right\}\delta_{n=\ell} \qquad (A-16)$$

$$C'_{k,m} = \frac{c}{2}\,\frac{t}{R}\,\frac{\beta_n^2}{\overline{\gamma}_{H,k,\ell}}\left\{\sum_{i=1}^{N_1} a_i^2(W_{io}+\overline{W}_{io})(\delta_{k=i+m}-\delta_{k=i-m})\right\}\delta_{n=\ell}$$

$$A''_{k,m} = \frac{-4}{\pi}\,c\,\frac{R}{t}\left\{\sum_{p,q=1}^{N_2}(W_{pq}+\overline{W}_{pq})(\phi_1\delta_{k\pm|m-p|=\text{odd}}\,\delta_{\ell=n+q}\right.$$

$$\left.-\phi_2\delta_{k\pm(m+p)=\text{odd}}\,\delta_{\ell=|n-q|})\right\}$$

$$B''_{k,m} = \frac{-4}{\pi}\,c\,\frac{R}{t}\left\{\sum_{p,q=1}^{N_2} F_{pq}(\phi_1\delta_{k\pm|m-p|=\text{odd}}\,\delta_{\ell=n+q}\right. \qquad (A-17)$$

$$\left.-\phi_2\delta_{k\pm(m+p)=\text{odd}}\,\delta_{\ell=|n-q|})\right\}$$

$$C''_{k,m} = \frac{c}{\pi}\,\frac{t}{R}\,\frac{1}{\overline{\gamma}_{H,k,\ell}}\left\{\sum_{p,q=1}^{N_2}(W_{pq}+\overline{W}_{pq})(\phi_1\delta_{k\pm|m-p|=\text{odd}}\,\delta_{\ell=n+q}\right.$$

$$\left.-\phi_2\delta_{k\pm(m+p)=\text{odd}}\,\delta_{\ell=|n-q|})\right\}$$

$$A_{k,k} = 2\frac{R}{t}(\overline{\gamma}_{Q,k,\ell} + a_k^2)$$

$$B_{k,k} = \overline{\gamma}_{D,k,\ell} - 2a_k^2\lambda \qquad \text{(A-18)}$$

$$C_{k,k} = -\frac{1}{2}\frac{t}{R}\frac{1}{\overline{\gamma}_{H,k,\ell}}(\overline{\gamma}_{Q,k,\ell} + a_k^2)$$

where $k, m = 1, 2, \ldots, N_2$

$$A_{k,m'} = \frac{4}{\pi} c \frac{R}{t}\left\{\sum_{p,q=1}^{N_3}\sum (W'_{pq}+\overline{W}'_{pq})(\phi_1\delta_{k\pm}|m'-p| = \text{odd}\,\delta_{\ell=n'+q} + \phi_2\delta_{k\pm(m'+p)=\text{odd}}\,\delta_{\ell=|n'-q|})\right\}$$

$$B_{k,m'} = \frac{4}{\pi} c \frac{R}{t}\left\{\sum_{p,q=1}^{N_3}\sum F'_{pq}(\phi_1\delta_{k\pm}|m'-p| = \text{odd}\,\delta_{\ell=n'+q} + \phi_2\delta_{k\pm(m'+p)=\text{odd}}\,\delta_{\ell=|n'-q|})\right\} \qquad \text{(A-19)}$$

$$C_{k,m'} = \frac{-c}{\pi}\frac{t}{R}\frac{1}{\overline{\gamma}_{H,k,\ell}}\left\{\sum_{p,q=1}^{N_3}\sum (W'_{pq}+\overline{W}'_{pq})(\phi_1\delta_{k\pm}|m'-p| = \text{odd}\,\delta_{\ell=n'+q} + \phi_2\delta_{k\pm(m'+p)=\text{odd}}\,\delta_{\ell=|n'-q|})\right\}$$

where $k = 1, 2, \ldots N_2$

$m' = 1, 2, \ldots, N_3$

$$E_{k\ell}^{(1)} = -\Bigg\{\frac{c}{4}\frac{t}{R}\frac{1}{\bar{\gamma}_{H,k,\ell}}\Bigg\langle\Bigg\langle\sum_{i=1}^{N_1}\alpha_i^2 W_{io}\Bigg\{\sum_{p,q=1}^{N_2}\beta_q^2(W_{pq}+2\overline{W}_{pq})(\delta_{k=i+p}-\delta_{k=|i-p|})\delta_{q=\ell}\Bigg\}\Bigg\rangle\Bigg\rangle$$

$$+\frac{c}{4}\frac{t}{R}\frac{1}{\bar{\gamma}_{H,k,\ell}}\Bigg\langle\Bigg\langle\sum_{p,q=1}^{N_2}\beta_q^2 W_{pq}\Bigg\{\sum_{i=1}^{N_1}\alpha_i^2(W_{io}+2\overline{W}_{io})(\delta_{k=i+p}-\delta_{k=|i-p|})\delta_{q=\ell}\Bigg\}\Bigg\rangle\Bigg\rangle$$

$$+\frac{1}{2}\frac{c}{\pi}\frac{t}{R}\frac{1}{\bar{\gamma}_{H,k,\ell}}\Bigg\langle\Bigg\langle\sum_{m,n=1}^{N_2}W_{mn}\Bigg\{\sum_{p,q=1}^{N_2}(W_{pq}+2\overline{W}_{pq})(\phi_1\delta_{k\pm|m-p|=\text{odd}}\delta_{\ell=n+q}$$

$$-\phi_2\delta_{k\pm(m+p)=\text{odd}}\delta_{\ell=|n-q|})\Bigg\}\Bigg\rangle\Bigg\rangle$$

$$-\frac{1}{2}\frac{c}{\pi}\frac{t}{R}\frac{1}{\bar{\gamma}_{H,k,\ell}}\Bigg\langle\Bigg\langle\sum_{m',n'=1}^{N_2}W'_{mn}\Bigg\{\sum_{p,q=1}^{N_3}(W'_{pq}+2\overline{W}'_{pq})(\phi_1\delta_{k\pm|m'-p|=\text{odd}}\delta_{\ell=n'+q}$$

$$+\phi_2\delta_{k\pm(m'+p)=\text{odd}}\delta_{\ell=|n'-q|})\Bigg\}\Bigg\rangle\Bigg\rangle$$

$$+F_{k\ell}\,\frac{-1}{2}\frac{t}{R}\frac{1}{\bar{\gamma}_{H,k,\ell}}+(\bar{\gamma}_{Q,k,\ell}+\alpha_k^2)\,W_{k\ell}\Bigg\} \qquad (A-20)$$

$$E_{k\ell}^{(2)} = -\Bigg\{-2c\,\frac{R}{t}\Bigg\langle\Bigg\langle\sum_{i=1}^{N_1}\alpha_i^2 F_{io}\Bigg\{\sum_{p,q=1}^{N_2}\beta_q^2(W_{pq}+\overline{W}_{pq})(\delta_{k=i+p}-\delta_{k=|i-p|})\delta_{q=\ell}\Bigg\}\Bigg\rangle\Bigg\rangle$$

$$-2c\,\frac{R}{t}\Bigg\langle\Bigg\langle\sum_{i=1}^{N_1}\alpha_i^2(W_{io}+\overline{W}_{io})\Bigg\{\sum_{p,q=1}^{N_2}\beta_q^2 F_{pq}(\delta_{k=i+p}-\delta_{k=|i-p|})\delta_{q=\ell}\Bigg\}\Bigg\rangle\Bigg\rangle$$

- .....

$$-\frac{4}{\pi} c \frac{R}{t} \left\langle \sum_{m,\, n=1}^{N_2}{}' F_{mn} \left\{ \sum_{p,\, q=1}^{N_2}{}' (W_{pq}+\overline{W}_{pq}) \left(\phi_1 \delta_{k\pm |m-p| = \text{odd}} \delta_{\ell = n+q} \right.\right.\right.$$

$$\left.\left.\left. -\phi_2 \, \delta_{k\pm (m+p) = \text{odd}} \delta_{\ell = |n-q|} \right) \right\} \right\rangle$$

$$+ \frac{4}{\pi} c \frac{R}{t} \left\langle \sum_{m',\, n'=1}^{N_3}{}' F'_{mn} \left\{ \sum_{p,\, q=1}^{N_3}{}' (W'_{pq}+\overline{W}'_{pq}) \left(\phi_1 \delta_{k\pm |m'-p| = \text{odd}} \delta_{\ell = n'+q} \right.\right.\right.$$

$$\left.\left.\left. +\phi_2 \delta_{k\pm (m'+p) = \text{odd}} \delta_{\ell = |n'-q|} \right) \right\} \right\rangle$$

$$+ 2 \frac{R}{t} (\bar{\gamma}_{Q,\, k,\, \ell} + \alpha_k^2) \, F_{k\ell} + \bar{\gamma}_{D,\, k,\, \ell} \, W_{k\ell} - 2\alpha_k^2 \lambda (W_{k\ell} + \overline{W}_{k\ell}) \Bigg\} \qquad \text{(A-21)}$$

where $k = 1, 2, \ldots, N_2$

$$A_{k',\, i} = -2 c \frac{R}{t} \alpha_i^2 \left\{ \sum_{p,\, q=1}^{N_3}{}' \beta_q^2 (W'_{pq}+\overline{W}'_{pq}) (\delta_{k' = i+p} - \delta_{k' = |i-p|}) \delta_{q=\ell'} \right\}$$

$$B_{k',\, i} = -2c \frac{R}{t} \alpha_i^2 \left\{ \sum_{p,\, q=1}^{N_3}{}' \beta_q^2 \, F'_{pq} \, (\delta_{k' = i+p} - \delta_{k' = |i-p|}) \, \delta_{q=\ell'} \right\}$$

$$C_{k',\, i} = \frac{c}{2} \frac{t}{R} \alpha_i^2 \, \frac{1}{\bar{\gamma}_{H,\, k',\, \ell'}} \left\{ \sum_{p,\, q=1}^{N_3}{}' \beta_q^2 (W'_{pq}+\overline{W}'_{pq}) (\delta_{k' = i+p} - \delta_{k' = |i-p|}) \, \delta_{q=\ell'} \right\}$$

where $k' = 1, 2, \ldots, N_3$

$i = 1, 2, \ldots, N_1$ (A-22)

$$A_{k',m} = \frac{-4}{\pi} c \frac{R}{t} \left\{ \sum_{p,q=1}^{N_3} (W'_{pq} + \overline{W}'_{pq})(\phi_1 \delta_{k' \pm |m-p|=\text{odd}} \delta_{\ell'=n+q} \right.$$

$$\left. + \phi_2 \delta_{k' \pm (m+p)=\text{odd}} \delta_{\ell'=|n-q|} \right\}$$

$$B_{k',m} = \frac{-4}{\pi} c \frac{R}{t} \left\{ \sum_{p,q=1}^{N_3} F'_{pq} (\phi_1 \delta_{k' \pm |m-p|=\text{odd}} \delta_{\ell'=n+q} \right.$$

$$\left. - \phi_2 \delta_{k' \pm (m+p)=\text{odd}} \delta_{\ell'=|n-q|} \right\}$$

$$C_{k',m} = \frac{c}{\pi} \frac{t}{R} \frac{1}{\overline{\gamma}_{H,k',\ell'}} \left\{ \sum_{p,q=1}^{N_3} (W'_{pq} + \overline{W}'_{pq})(\phi_1 \delta_{k' \pm |m-p|=\text{odd}} \delta_{\ell'=n+q} \right.$$

$$\left. + \phi_2 \delta_{k' \pm (m+p)=\text{odd}} \delta_{\ell'=|n-q|} \right\} \qquad \text{(A-23)}$$

where $k' = 1, 2, \ldots, N_3$

$m = 1, 2, \ldots, N_2$

$$A_{k',m'} = A'_{k',m'} + A''_{k',m'} + A_{k',k'} \delta_{k'=m'}$$

$$B_{k',m'} = B'_{k',m'} + B''_{k',m'} + B_{k',k'} \delta_{k'=m'}$$

$$C_{k',m'} = C'_{k',m'} + C''_{k',m'} + C_{k',k'} \delta_{k'=m'} \qquad \text{(A-24)}$$

where

$$A'_{k',m'} = -2\,c\,\frac{R}{t}\,\beta^2_{n'}\left\{\sum_{i=1}^{N_1} a_i^2(W_{io}+\overline{W}_{io})(\delta_{k'=i+m'}-\delta_{k'=|i-m'|})\right\}\delta_{n'=\ell'}$$

$$B'_{k',m'} = -2\,c\,\frac{R}{t}\,\beta^2_{n'}\left\{\sum_{i=1}^{N_1} a_i^2 F_{io}(\delta_{k'=i+m'}-\delta_{k'=|i-m'|})\right\}\delta_{n'=\ell'} \qquad (A-25)$$

$$C'_{k',m'} = \frac{c}{2}\,\frac{t}{R}\,\frac{\beta^2_{n'}}{\overline{\gamma}_{H,k',\ell'}}\left\{\sum_{i=1}^{N_1} a_i^2(W_{io}+\overline{W}_{io})(\delta_{k'=i+m'}-\delta_{k'=|i-m'|})\right\}\delta_{n'=\ell'}$$

$$A''_{k',m'} = \frac{-4}{\pi}\,c\,\frac{R}{t}\left\{\sum_{p,q=1}^{N_2}(W_{pq}+\overline{W}_{pq})(\phi_1\delta_{k'\pm|m'-p|=\text{odd}}\delta_{\ell'=n'+q} - \phi_2\delta_{k'\pm(m'+p)=\text{odd}}\delta_{\ell'=|n'-q|})\right\}$$

$$B''_{k',m'} = \frac{-4}{\pi}\,c\,\frac{R}{t}\left\{\sum_{p,q=1}^{N_2} F_{pq}(\phi_1\delta_{k'\pm|m'-p|=\text{odd}}\delta_{\ell'=n'+q} + \phi_2\delta_{k'\pm(m'+p)=\text{odd}}\delta_{\ell'=|n'-q|})\right\} \qquad (A-26)$$

$$C''_{k',m'} = \frac{c}{\pi}\,\frac{t}{R}\,\frac{1}{\overline{\gamma}_{H,k',\ell'}}\left\{\sum_{p,q=1}^{N_2}(W_{pq}+\overline{W}_{pq})(\phi_1\delta_{k'\pm|m'-p|=\text{odd}}\delta_{\ell'=n'+q} - \phi_2\delta_{k'\pm(m'+p)=\text{odd}}\delta_{\ell'=|n'-q|})\right\}$$

$$A_{k',k'} = 2\,\frac{R}{t}(\overline{\gamma}_{Q,k',\ell'}+a^2_{k'})$$

$$B_{k',k'} = \overline{\gamma}_{D,k',\ell'}-2a^2_{k'}\lambda \qquad (A-27)$$

$$C_{k',k'} = \frac{-1}{2}\,\frac{t}{R}\,\frac{1}{\overline{\gamma}_{H,k',\ell'}}\,(\overline{\gamma}_{Q,k',\ell'}+a^2_{k'})$$

where $k', m' = 1, 2, \ldots, N_3$

$$E^{(1)}_{k'\ell'} = -\Bigg\{\frac{c}{4}\frac{t}{R}\frac{1}{\bar{\gamma}_{H,k',\ell'}}\Bigg\langle \sum_{i=1}^{N_1} a_i^2 W_{io}\Bigg\{\sum_{p,q=1}^{N_3\,N_3}\beta_q^2(W'_{pq}+2\overline{W}'_{pq})(\delta_{k'=i+p}-\delta_{k'=|i-p|})\,\delta_{q=\ell'}\Bigg\rangle$$

$$+\frac{c}{4}\frac{t}{R}\frac{1}{\bar{\gamma}_{H,k',\ell'}}\Bigg\langle \sum_{m',n'=1}^{N_3\,N_3}\beta_{n'}^2 W'_{mn}\Bigg\{\sum_{i=1}^{N_1} a_i^2(W_{io}+2\overline{W}_{io})(\delta_{k'=i+m'}-\delta_{k'=i-m'})\Bigg\}\delta_{n'=\ell'}\Bigg\rangle$$

$$+\frac{1}{2}\frac{c}{\pi}\frac{t}{R}\frac{1}{\bar{\gamma}_{H,k',\ell'}}\Bigg\langle \sum_{m,n=1}^{N_2\,N_2} W_{mn}\Bigg\{\sum_{p,q=1}^{N_3\,N_3}(W'_{pq}+2\overline{W}'_{pq})(\phi_1\delta_{k'\pm|m-p|=\text{odd}}\,\delta_{\ell'=n+q}$$

$$+\phi_2\delta_{k'\pm(m+p)=\text{odd}}\,\delta_{\ell'=|n-q|})\Bigg\}\Bigg\rangle$$

$$+\frac{1}{2}\frac{c}{\pi}\frac{t}{R}\frac{1}{\bar{\gamma}_{H,k',\ell'}}\Bigg\langle \sum_{m',n'=1}^{N_3\,N_3} W'_{mn}\Bigg\{\sum_{p,q=1}^{N_2\,N_2}(W_{pq}+2\overline{W}_{pq})(\phi_1\delta_{k'\pm|m'-p|=\text{odd}}\,\delta_{\ell'=n'+q}$$

$$+\phi_2\delta_{k'\pm(m'+p)=\text{odd}}\,\delta_{\ell'=|n'-q|})\Bigg\}\Bigg\rangle$$

$$+F_{k'\ell'}\,\frac{-1}{2}\frac{t}{R}\frac{1}{\bar{\gamma}_{H,k',\ell'}}(\bar{\gamma}_{Q,k',\ell'}+a_{k'}^2)W_{k'\ell'}\Bigg\} \qquad \text{(A-28)}$$

$$E^{(2)}_{k'\ell'} = -\Bigg\{-2c\,\frac{R}{t}\Bigg\langle \sum_{i=1}^{N_1} a_i^2 F_{io}\Bigg\{\sum_{p,q=1}^{N_3\,N_3}\beta_q^2(W'_{pq}+\overline{W}'_{pq})(\delta_{k'=i+p}-\delta_{k'=|i-p|})\delta_{q=\ell'}\Bigg\}\Bigg\rangle$$

$$-2c\,\frac{R}{t}\Bigg\langle \sum_{i=1}^{N_1} a_i^2(W_{io}+\overline{W}_{io})\Bigg\{\sum_{p,q=1}^{N_3\,N_3}\beta_q^2 F'_{pq}\,(\delta_{k'=i+p}-\delta_{k'=|i-p|})\,\delta_{q=\ell'}\Bigg\}\Bigg\rangle$$

- .....

$$-\frac{4}{\pi}\,c\,\frac{R}{t}\left\langle \sum_{m,\,n=1}^{N_2}{}' F_{mn}\left\{ \sum_{p,\,q=1}^{N_3}(W'_{pq}+\overline{W}'_{pq})(\phi_1\delta_{k'\pm|m-p|=\text{odd}}\,\delta_{\ell'=n+q}\right.\right.$$

$$\left.\left.+\phi_2\delta_{k'\pm(m+p)=\text{odd}}\,\delta_{\ell'=|n-q|}\right)\right\}\right\rangle$$

$$-\frac{4}{\pi}\,c\frac{R}{t}\left\langle \sum_{m',\,n'=1}^{N_3}{}' F'_{mn}\left\{ \sum_{p,\,q=1}^{N_2}(W_{pq}+\overline{W}_{pq})(\phi_1\delta_{k'\pm|m'-p|=\text{odd}}\,\delta_{\ell'=n'+q}\right.\right.$$

$$\left.\left.+\phi_2\delta_{k'\pm(m'+p)=\text{odd}}\,\delta_{\ell'=|n'-q|}\right)\right\}\right\rangle$$

$$+\,2\,\frac{R}{t}(\overline{\gamma}_{Q,k',\ell'}+\alpha^2_{k'})\,F_{k'\ell'}+\overline{\gamma}_{D,k',\ell'}W_{k'\ell'}-2\alpha^2_{k'}\lambda(W_{k'\ell'}+\overline{W}'_{k'\ell'})\Big\}$$

$$\text{where } k' = 1, 2, \ldots, N_3 \qquad \text{(A-29)}$$

The stiffener parameters $\overline{\gamma}_{H,k,\ell}$, $\overline{\gamma}_{D,k,\ell}$, $\overline{\gamma}_{Q,k,\ell}$.... etc. and the wave parameters α_i^2, β_n^2,... etc. are defined in Reference 11. Other special symbols used in this appendix are Kronecker deltas like:

$$\begin{aligned}
\delta_{k'=i+p} &= 1 \quad \text{if} \quad k' = i+p \\
&= 0 \quad \text{if} \quad k' \neq i+p \\
\delta_{k'=|i-p|} &= 1 \text{ if} \quad k' = |i-p| \\
&= 0 \text{ if} \quad k' \neq |i-p|
\end{aligned} \qquad \text{A-30)}$$

....

....

Also

$$\phi_1 = \frac{\bar{a}_1 k}{k^2-(m-p)^2} - \frac{\bar{a}_2 k}{k^2-(m+p)^2} \quad \text{if} \quad k \pm |m-p| = \text{odd}$$

$$= 0 \qquad \text{otherwise} \tag{A-31}$$

$$\phi_2 = \frac{\bar{a}_1 k}{k^2-(m+p)^2} - \frac{\bar{a}_2 k}{k^2-(m-p)^2} \quad \text{if} \quad k \pm (m+p) = \text{odd}$$

$$= 0 \qquad \text{otherwise} \tag{A-32}$$

where

$$\bar{a}_1 = (a_m \beta_q + a_p \beta_n)^2$$
$$\bar{a}_2 = (a_m \beta_q - a_p \beta_n)^2 \tag{A-33}$$

APPENDIX B

DERIVATION OF THE PERIODICITY CONDITION

In order to satisfy periodicity in the circumferential direction, the solution must satisfy the following equation:

$$\int_0^{2\pi R} v_{,y}\, dy = 0 \tag{B-1}$$

where

$$v_{,y} = \epsilon_y - \left[-\frac{1}{R} W + \frac{1}{2}\left(W_{,y} + 2\overline{W}_{,y}\right) W_{,y}\right]$$

$$\epsilon_y = \frac{\overline{H}_{xx}}{Et}\left(F_{,xx} - \frac{\nu}{1+\mu_1} F_{,yy}\right) + (1+\mu_1)\hat{\beta}\chi_2 W_{,yy} - \nu\hat{\beta}\chi_1 W_{,xx} \tag{B-2}$$

Substituting for $\overline{W}$, W and F the assumed double Fourier series (Eqs. (12), (13) and (14)), carrying out the y-integration, regrouping and introducing the usual nondimensional parameters, yields:

$$\sum_{i=1}^{N_1}\left\{-2a_i^2\,\overline{H}_{xx} F_{io} + \frac{t}{R}\left(\overline{Q}_{xx} a_i^2 + 1\right) W_{io}\right\}\cos\frac{i\pi x}{L} + \frac{t}{R}\left(\frac{\overline{H}_{xx}}{1+\mu_1}\,\frac{\nu\lambda}{c} + W_\nu\right)$$

$$-\frac{t}{R}\,\frac{c}{4}\sum_{k,\ell=1}^{N_2}{}' \sum_{m,n=1}^{N_2} \beta_\ell \beta_n \left(W_{k\ell} + 2\overline{W}_{k\ell}\right) W_{mn}\left[\cos(k-m)\frac{\pi x}{L} - \cos(k+m)\frac{\pi x}{L}\right]\delta_{n=\ell}$$

$$-\frac{t}{R}\,\frac{c}{4}\sum_{k',\ell'=1}^{N_3}\sum_{m',n'=1}^{N_3} \beta_{\ell'} \beta_{n'} \left(W'_{k\ell} + 2\overline{W}'_{k\ell}\right) W'_{mn}\left[\cos(k'-m')\frac{\pi x}{L} - \cos(k'+m')\frac{\pi x}{L}\right]\delta_{n'=\ell'}$$

$$= \epsilon_\delta \tag{B-3}$$

This expression does not hold in general; however, in the sense of Galerkin's approximation we may require that

$$\int_0^L \epsilon_\delta \cos \frac{j\pi x}{L} \, dx = 0 \tag{B-4}$$

Also we let:

$$W_\nu = - \frac{\nu}{c} \frac{\overline{H}_{xx}}{1+\mu_1} \lambda \tag{B-5}$$

Carrying out the integral and regrouping the resulting expression yields:

$$F_{io} - \frac{1}{2} \frac{t}{R} \frac{(\overline{Q}_{xx} a_i^2 + 1)}{a_i^2 \overline{H}_{xx}} W_{io}$$

$$- \frac{c}{8} \frac{t}{R} \frac{1}{a_i^2 \overline{H}_{xx}} \left\langle \sum_{k,\ell=1}^{N_2} \beta_\ell W_{k\ell} \left\{ \sum_{p,q=1}^{N_2} \beta_q (W_{pq} + 2\overline{W}_{pq}) (\delta_{i=k+p} - \delta_{i=|k-p|}) \delta_{q=\ell} \right\} \right\rangle$$

$$- \frac{c}{8} \frac{t}{R} \frac{1}{a_i^2 \overline{H}_{xx}} \left\langle \sum_{k',\ell'=1}^{N_3} \beta_{\ell'} W'_{k\ell} \left\{ \sum_{p,q=1}^{N_3} \beta_q (W'_{pq} + 2\overline{W}'_{pq}) (\delta_{i=k'+p} - \delta_{i=|k-p|}) \delta_{q=\ell'} \right\} \right\rangle = 0 \tag{B-6}$$

But this equation is identically equal to the axisymmetric part of the compatibility equation (A-12).

Thus the converged solutions, which satisfy the compatibility equation in the sense of Galerkin, also satisfy the circumferential periodicity condition to the same approximation.

Shell	$t \times 10^3$	R/t	L/R	A/dt	-e/t	I/dt^3	d	L	$E \times 10^{-6}$	No. of Stiffeners
X-1	4.00	1000	1.00	-	-	-	-	1.0	15.2	-
A-8	4.64	862	2.00	-	-	-	-	8.0	15.2	-
B-1	8.07	496	1.94	-	-	-	-	7.75	15.45	-
XR-1	9.29	431	1.00	0.205	1.13	0.0288	0.250	4.0	10.0	14
AR-1	9.29	431	1.31	0.205	1.13	0.0288	0.250	5.25	10.0	20
XS-1	7.74	517	1.00	0.506	1.71	0.2466	0.316	4.0	10.0	80
AS-2	7.74	517	1.38	0.506	1.71	0.2466	0.316	5.5	10.0	80

All dimensions in inches, unless otherwise indicated. $\nu = 0.3$.

TABLE I. GEOMETRIC AND MATERIAL PROPERTIES OF THE SHELLS

	N_{x_M}			$N_{x_{NL}}$		
Shell	SS-3	C-3	C-4	SS-3	C-3	C-4
X-1	37.0 (13)	37.3 (27)	36.8 (ℓ)[1]	31.0 (26)	33.4 (26)	34.0 (27)
A-8	49.6 (9)	50.0 (9)	49.5 (ℓ)[1]	41.3 (24)	44.8 (24)	45.7 (ℓ)[1]
B-1	152.7 (8)	154.1 (8)	152.2 (ℓ)[1]	127.2 (18)	137.7 (18)	140.6 (ℓ)[1]
XR-1	142.4 (0)	143.8 (0)	143.8 (0)	135.3 (12)	142.2 (9)	143.1 (13)
AR-1	142.5 (0)	143.2 (0)	143.1 (0)	135.0 (13)	141.8 (7)	142.6 (11)
XS-1	141.6 (11)	161.6 (12)	204.0 (16)	134.4 (11)	160.2 (12)	197.1 (16)
AS-2	131.2 (10)	146.7 (10)	183.2 (14)	127.9 (10)	146.4 (10)	180.9 (14)

Numbers in parentheses are the number of circumferential waves, ℓ

N_{x_M} = Buckling load from BOSOR[19] or SRA[20] using membrane prebuckling analysis (lb/in)

$N_{x_{NL}}$ = Buckling load from BOSOR[19] or SRA[20] using nonlinear prebuckling analysis (lb/in)

SS-3 - $w = M_x = v = N_x = 0$

C-3 - $w = w_{,x} = v = N_x = 0$

C-4 - $w = w_{,x} = v = u = 0$

[1]Values taken from Reference 23

TABLE II. BUCKLING LOADS OF THE PERFECT SHELLS

	X-1		XR-1		XS-1	
	SS-3	C-3	SS-3	C-3	SS-3	C-3
N_{x_M}	37.0 (13)	37.3 (27)	142.4(0)	143.8 (0)	141.6 (11)	161.6 (12)
$N_{s_{MM}}$	24.8 (13)	-	123.4 (9)	-	88.3 (11)	-
$N_{s_{EXT}}$	-	24.6 (13)	-	119.2 (9)	87.7 (11)	102.5 (11)
$\frac{N_{s_{MM}}}{N_{x_M}}$	0.67	-	0.87	-	0.62	-
$\frac{N_{s_{EXT}}}{N_{x_M}}$		0.66	-	0.83	-	0.63

Numbers in parentheses are the number of circumferential waves, ℓ

N_{x_M} = Buckling load from BOSOR[19] or SRA[20] using membrane prebuckling analysis (lb/in)

$N_{s_{MM}}$ = Imperfect shell buckling load by the multimode analysis

$N_{s_{EXT}}$ = Imperfect shell buckling load by the extended[24, 25] analysis

TABLE III. BUCKLING LOADS OF THE IMPERFECT SHELLS

	Cosine Representation Axisymmetric		Sine Representation Asymmetric		
	$\overline{X}_A$	q	$\overline{X}$	r	s
A-8	0.1280	1.18	1.630	1.01	1.33
B-1	0.1780	1.43	0.960	1.13	1.18
AR-1	0.0208	1.50	0.206	1.18	1.22
AS-2	0.0068	0.25	0.786	1.12	1.23

TABLE IV. IMPERFECTION MODEL SUMMARY

2-modes	ρ_s
(2, 0) + (1. 9)	= 0. 901
4-modes	
(2, 0)+(1, 9)+(33, 9)+(34, 0)	= 0. 846
6-modes	
(33, 7) / (33, 2) / (2, 0)+(1, 9)+(33, 9)+(34, 0)	= 0. 763
8-modes	
(1, 7) (33, 7) / (1, 2) (33, 2) / (2, 0)+(1, 9)+(33, 9)+(34, 0)	= 0. 744

10-modes	ρ_s
(1, 11) (1, 7) (33, 11) (33, 7) / (1, 2) (33, 2) / (2, 0)+(1, 9)+(33, 9)+(34, 0)	= 0. 699
15-modes	
(1, 11) (1, 7) (33, 11) (33, 7) / (1, 2) (33, 2) / (2, 0)+(1, 9)+(33, 9)+(34, 0) / (2, 4) (32, 4) / (4, 0)+(2, 13)+(32, 13)+(34, 0)	= 0. 693

TABLE V. BUCKLING LOADS CALCULATED BY THE MULTIMODE ANALYSIS (SHELL A-8)

2-modes	ρ_s
(2, 0)+(1, 8)	= 0. 837
4-modes	
(2, 0)+(1, 8)+(25, 8)+(26, 0)	= 0. 803

15-modes	ρ_s
(1, 10) (1, 6) (25, 10) (25, 6) / (1, 2) (25, 3) / (2, 0)+(1, 8) + (25, 8) + (26, 0) / (2, 3) (24, 3) / (4, 0)+(2, 11) + (24, 11) + (26, 0)	= 0. 663

TABLE VI. BUCKLING LOADS CALCULATED BY THE MULTIMODE ANALYSIS (SHELL B-1)

2-modes	ρ_s
(16, 0)+(8, 16)	= 0.995
4-modes	
(2, 0)+(1, 8)+(15, 8)+(16, 0)	= 0.985
6-modes	
(15, 6) | (15, 2) | (2, 0)+(1, 8)+(15, 8)+(16, 0)	= 0.965
8-modes	
(1, 6) (15, 6) | | (1, 2) (15, 2) | | (2, 0)+(1, 8)+(15, 8)+(16, 0)	= 0.959
12-modes	
(1, 6) (1, 5) (15, 6) (15, 5) | | | | (1, 2) (1, 3) (15, 2) (15, 3) \ | | / (2, 0)+(1, 8)+(15, 8)+(16, 0)	= 0.946
20-modes	
(1, 13) (15, 13) | | (1, 3) (15, 3) | | (1, 10) (15, 10) | | (1, 2) (15, 2) | | (2, 0)+(1, 8)+ (15, 8)+(16, 0) | | (1, 15) (15, 15) \ | | / (1, 9) (1, 7) (15, 7) (15, 9) | | (1, 6) (15, 6)	= 0.932

TABLE VII. BUCKLING LOADS CALCULATED BY THE MULTIMODE ANALYSIS (SHELL AR-1)

2-modes	ρ_s
(2, 0)+(1, 10)	= 0.904
4-modes	
(2, 0)+(1, 10)+(9, 10)+(10, 0)	= 0.903
14-modes	
(1, 19) (9, 19) | | (1, 9) (9, 9) | | (2, 0)+(1, 10)+(9, 10)+(10, 0) | | (1, 11) (9, 11) | | (1, 21) (9, 21) | | (1, 2) (9, 2)	= 0.824

TABLE VIII. BUCKLING LOADS CALCULATED BY THE MULTIMODE ANALYSIS (SHELL AS-2)

Shell	ρ_s	ρ_{EXP}	$\Delta\rho$
A-8	0.69	0.66	0.03
B-1	0.66	0.60	0.06
AR-1	0.93	0.81	0.12
AS-2	0.82	0.71	0.11

$$\rho_s = \frac{N_{s_{MM}}}{N_{x_{SS-3}}} \; ; \quad \rho_{EXP} = \frac{N_{x_{EXP}}}{N_{x_{C-4}}}$$

$N_{x_{SS-3}}$, $N_{x_{C-4}}$ = Perfect shell buckling loads using membrane prebuckling

TABLE IX. COMPARISON BETWEEN THEORY AND EXPERIMENTS

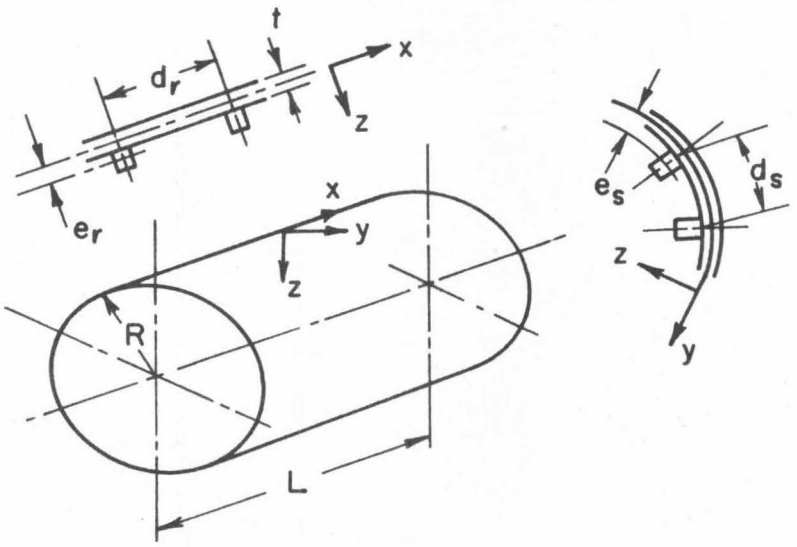

FIG. 1 NOTATION AND SIGN CONVENTION

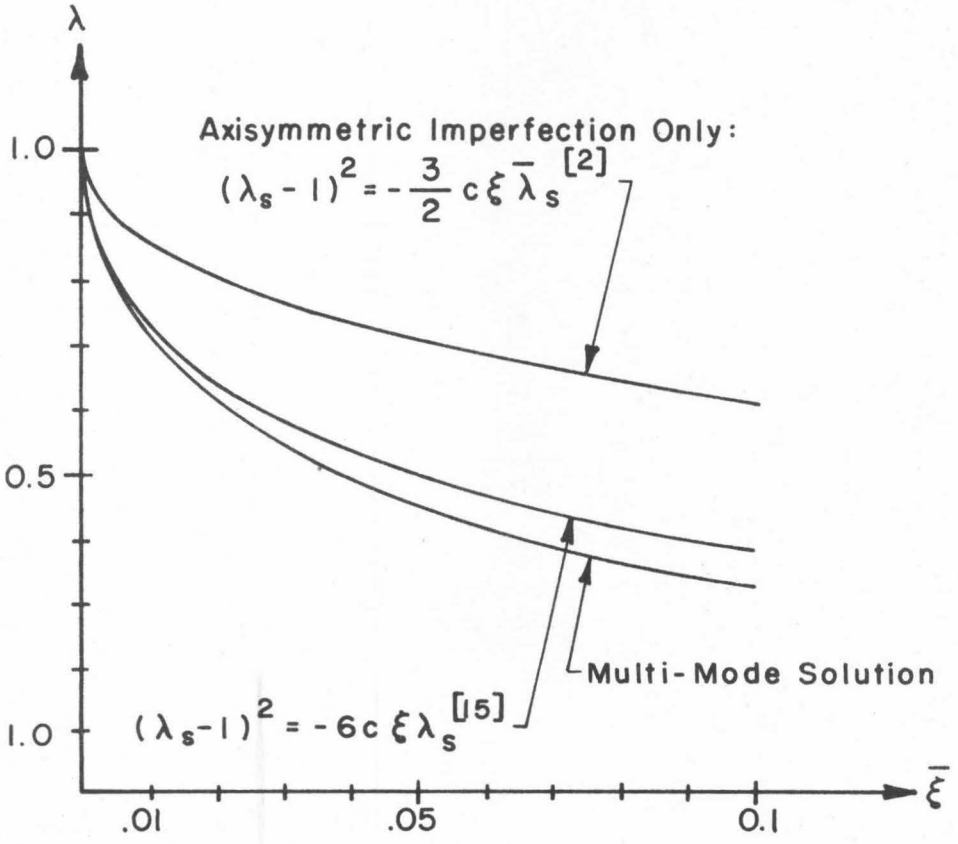

FIG. 2 COMPARISON OF BUCKLING LOAD PREDICTIONS FOR IMPERFECT SHELLS

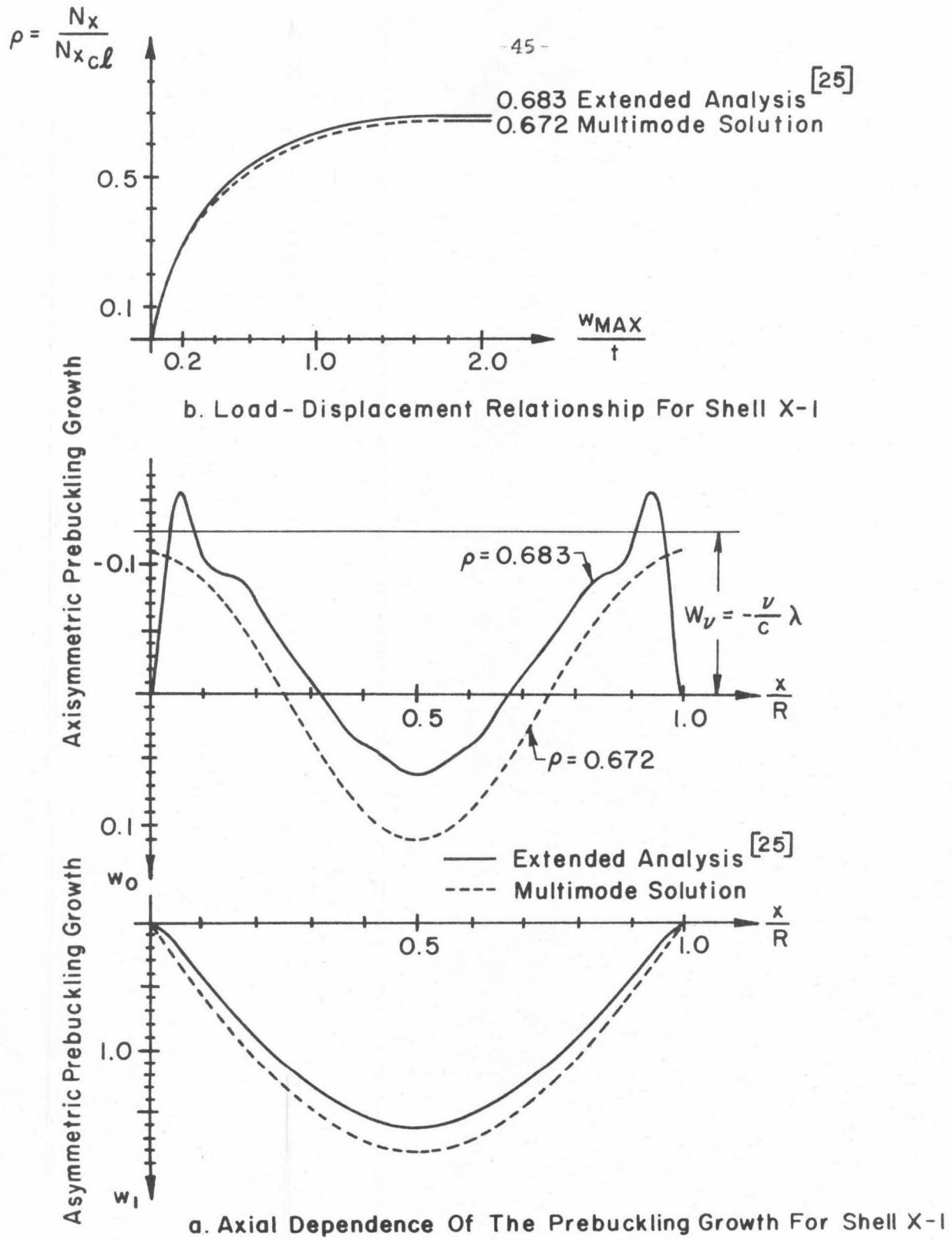

FIG. 3 COMPARISON BETWEEN MULTIMODE AND EXTENDED ANALYSES

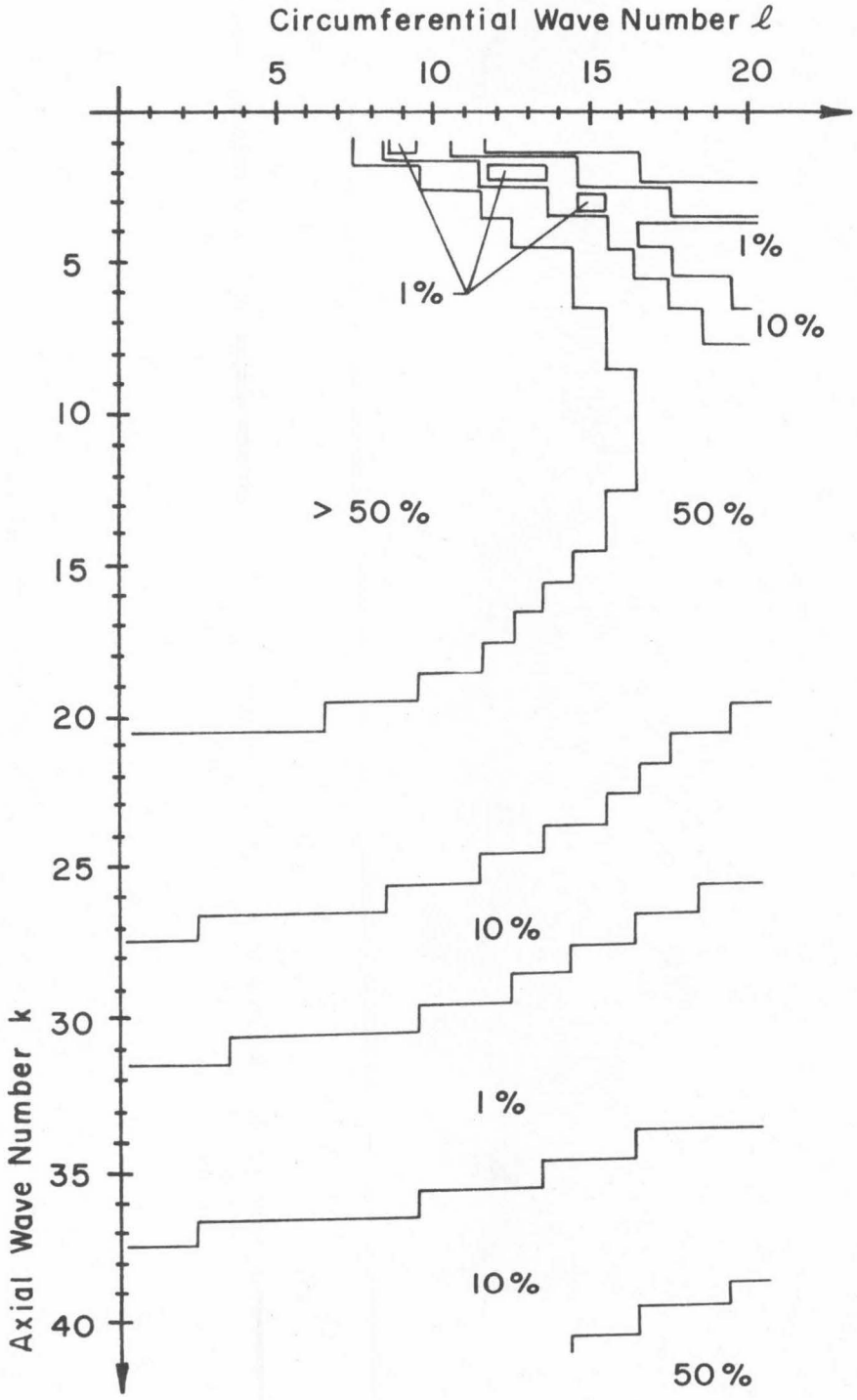

FIG. 4 BUCKLING LOADS FROM LINEAR THEORY FOR SHELL A-8 (SS-3 BOUNDARY CONDITION - $w = M_x = v = N_x = 0$)

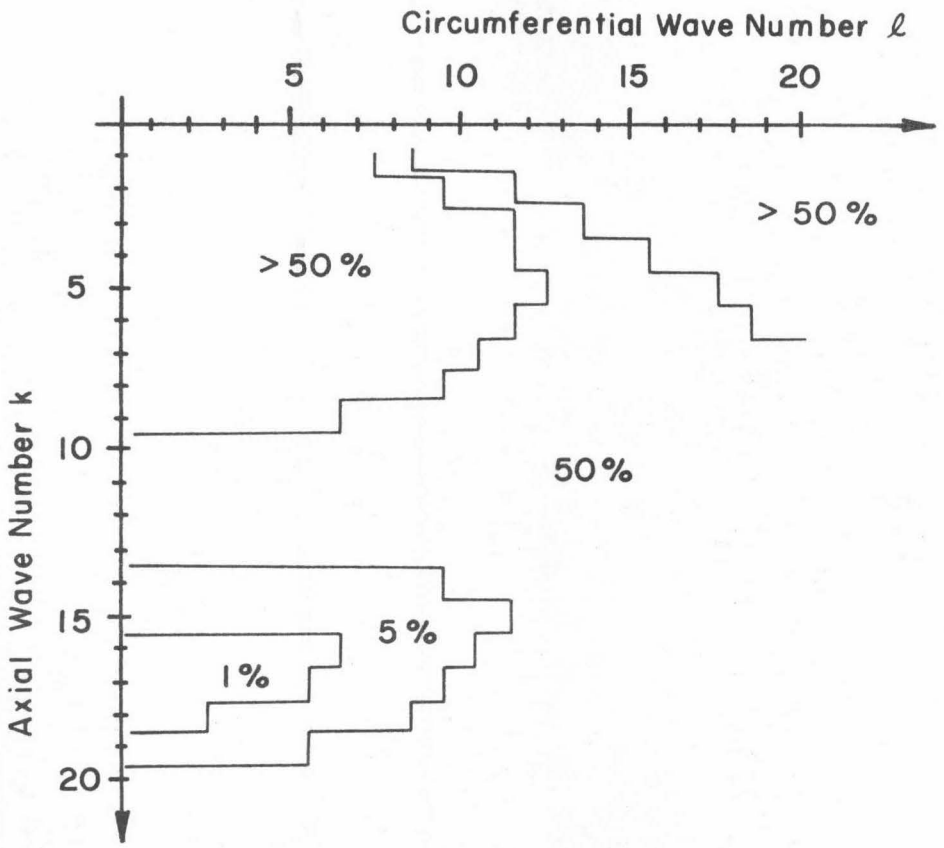

FIG. 5 BUCKLING LOADS FROM LINEAR THEORY FOR SHELL AR-1 (SS-3 BOUNDARY CONDITION - $w = M_x = v = N_x = 0$)

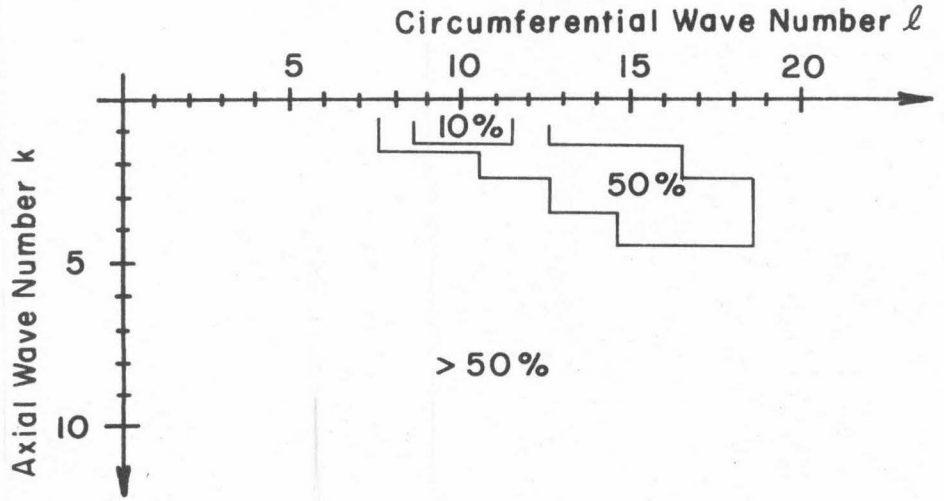

FIG. 6 BUCKLING LOADS FROM LINEAR THEORY FOR SHELL AS-2 (SS-3 BOUNDARY CONDITION - $w = M_x = v = N_x = 0$)